A fluid dynamics approach to motion control for rigid autonomous ground vehicles

Mengxuan Song, Nan Wang & Jun Wang
Department of Control Science and Engineering, Tongji University, Shanghai, PR China

Tim Gordon
University of Lincoln, Lincoln, UK

ABSTRACT: This paper concerns the low-speed maneuvering of autonomous ground vehicles. A novel guidance method is introduced based on the fluid flow analogy; in this approach, both path topology and motion reference are derived at a single step. Motion control then results from obtaining a best fit to the fluid motion distribution taking account of three constraints: boundary avoidance, rigidity of the vehicle and non-holonomic velocity constraints due to the steering system. Combined with weighted-least-squares fitting, an analytical solution is obtained for the steering angle. The methodology has the advantage of being applicable to both low-speed precision maneuvering and for dynamic control at highway speeds.

1 INTRODUCTION

The paper addresses the guidance and control of road vehicles requiring precise low-speed manoeuvring in complex environments, for example in autonomous freight operations where large vehicles operate within a limited motion space. In such cases the technical challenges are typically: (1) choosing the optimal (or at least feasible) path topology, i.e., decision making about which turns to make to reach the goal; (2) identifying a suitable reference path; (3) applying steering control, i.e., following the reference path, while respecting collision avoidance constraints with boundaries. The problem is made more complex when manoeuvring cars or trucks in narrow spaces, taking account of non-holonomic constraints from the wheel motions, which for low-speed maneuvers may be assumed to have zero sideslip angles.

Various navigation methods have been developed. Conventional graph search algorithms, such as Dijkstra (Dijkstra 1959), A* (Stentz 1994) and D* algorithm (Likhachev 2005), search the global map for a path. But the graph search algorithms are designed for holonomic systems.

Artificial intelligent algorithms including fuzzy logic algorithm (Saffiotti 1997), genetic algorithm and neural networks (Sedighi 2004) have been successfully implemented in the path planning problem. Artificial intelligence based algorithms can handle constraints of vehicle kinematics and environment, but solutions are not always available.

Conventional approaches such as Artificial Potential Field (APF) method (Hwang 1992) have been proposed to deal with geometrical constraints by introducing potential functions. APF method can provide smooth and collision-free paths. But local minima of the potential energy field may exist, making the APF method inappropriate for guidance.

Much recent research has been devoted to developing sampling based planners such as the Rapidly-exploring Randomized Tree method (LaValle 2001) and the Probabilistic Road Map method (Kavraki 1996). One of the key drawbacks of the sampling-based path planning method is that the probabilistic completeness is achieved only when the number of samples approaches infinity. Besides, they are also not appropriate for non-holonomic systems.

For a non-holonomic system such as a self-driving car, the kinematic constraints can render a path infeasible, and the feasibility highly depends on the configuration of the vehicle. For example, if the rear wheels are steerable, more paths will become feasible. In this paper we directly consider a novel and more direct technique inspired by the physics of fluid motions and consistent with previous work on high speed motion control (Gordon 2002, Gordon 2006), the aim being to define and evaluate a path planning and control methodology that can be efficient, modular, open to operator scrutiny and also seamless across different speed ranges. In this paper we introduce and test the underlying concept, restricting attention to low-speed manoeuvring.

2 METHODOLOGY

2.1 *Overview*

The proposed motion control method is inspired by the natural phenomenon that the fluid will always finds its way to the exit in a given environment with complex boundaries, if the conditions are properly set. The velocity field of the fluid ('flow field') is somehow providing a collection of ubiquitous signposts throughout the domain. With appropriately designed algorithms, this steering angle of the vehicle may be determined directly from the local velocity field, and the outcome would be possible to lead the vehicle to the designated target without performing the traditional path following control strategies. With the help of the local flow field, the motion control method will require no global information. Note that only the direction of the flow field matters for the motion control in the proposed method, its velocity magnitude is irrelevant.

2.2 *Settings of flow field simulation*

The flow field in the present study acts as a reference or guidance to the motion control of the vehicle. It is important for the flow field to have particular features: (1) completeness should be guaranteed, meaning that the fluid will always reach the destination no matter where it starts; (2) smoothness of the streamline, which makes the vehicle easier to follow; (3) laminar flow is required since the turbulence does nothing beneficial to our current goal. Note that the flow field need not represent all physical characteristics of real-world fluid motions.

Considering these requirements, we employ the CFD method to simulate the fluid motion and obtain the velocity field. The borders of the domain are set exactly to the geometry of the walls and obstacles that the vehicle may encounter. An inlet for fluid is defined right behind the vehicle at its initial state, while an outlet is defined in front of the vehicle at its expected final state. Since we are dealing with the ground vehicle on a horizontal surface, the two-dimensional laminar Navier-Stokes (NS) equations without gravity are chosen. Let $\mathbf{u}(\mathbf{x})$ be the velocity vector at the position $\mathbf{x}$; the mass conservation equation and the momentum conservation equation are

$$\nabla \mathbf{u} = 0 \tag{1}$$

$$\rho \mathbf{u} \cdot \nabla \mathbf{u} = -\nabla p + \nabla \cdot \left(\mu \nabla \mathbf{u} \right) \tag{2}$$

where ρ is the density of the fluid, p is the pressure, and μ is the viscosity of the fluid.

The mass conservation law will guarantee that streamlines, originating at the designated inlet point, will reach the outlet without ending prematurely. The Reynolds number is defined as $\mathrm{Re}=\rho UL/\mu$, where U is the characteristic velocity, and L is the characteristic length. If Re is extremely low, vortices can be excluded, and any streamline from within the domain is guaranteed to reach the outlet. With these features implemented, the flow field will provide information for the ground vehicle, guiding it back on track when it has been deviated from desired course.

To achieve this, the boundary conditions are set as follows. A constant velocity vector is given for the inlet boundary, with a sufficiently small magnitude (10^{-5}m/s in the present study), and a direction perpendicular to the inlet boundary itself. The outlet boundary is set as an outflow boundary without reflux. Domain and obstacle borders are treated as non-slip stationary walls.

The mesh is generated with ANSYS ICEM CFD to discretize the calculation domain, with the cell scale at roughly 0.5m. Blue lines in Figure 1 demonstrate an example of the mesh generation for a double-lane-change scenario. Three white rectangles represent three static obstacles. The simulated airflow enters the domain at X=0m and exits at X=50m. ANSYS Fluent is used to solve the NS equations and to obtain the velocity field. The calculated flow field contains a velocity vector at every node of the cells throughout the discretized domain, plotted as red arrows in Figure 1, where the length of the arrow represents the magnitude of the velocity vector. It can be seen that due to the friction of the walls and the viscosity of the fluid, velocity is much lower near the borders and the obstacles. Figure 2 shows several streamlines originating near the entrance, and the background contour color represents the velocity magnitude. Because of mass conservation, every portion of the fluid that enters the domain must leave through the exit. This demonstrates the 'search capability' of the ensemble of fluid particles.

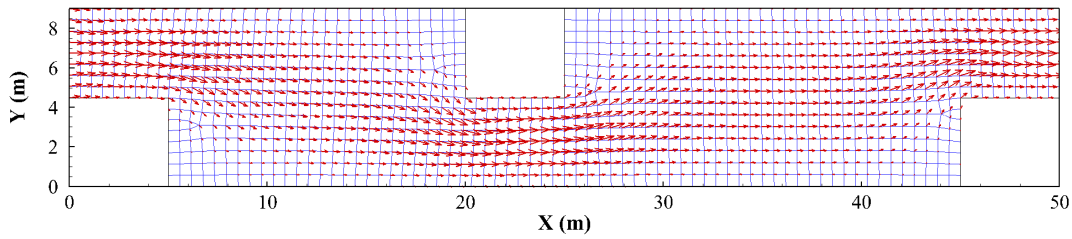

Figure 1. Simulated velocity vector field of a double lane change scenario

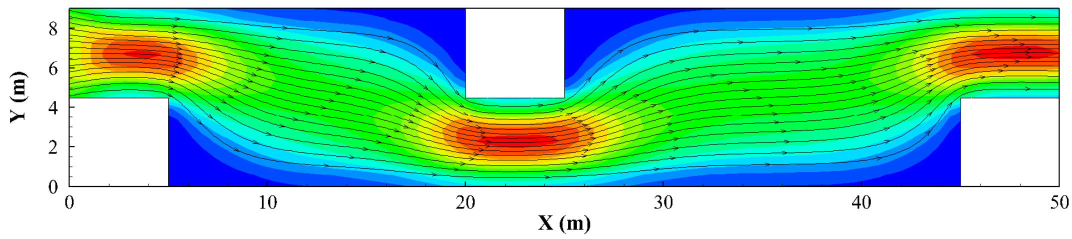

Figure 2. Simulated streamlines of a double lane change scenario

2.3 *Flow field guided motion control*

To conduct preliminary test and validation for the proposed flow field guided method, the simplest kinematic bicycle model is employed to consider and to simulate the movement of the vehicle. The centre of the rear axle is chosen as origin of the vehicle-based local coordinate system, x axis longitudinal and y axis lateral to the left (ISO convention). This is convenient as the origin serves as a 'pivot point' – with zero sideslip at the un-steered rear axle, the velocity vector always lies along the x axis. If V is the speed of the pivot point relative to the ground, and ω is the vehicle yaw rate, the velocity vector of any point i on the vehicle body is (V-ωy_i, ωx_i). Note that ω is constrained by a limitation of minimum turning radius $R_{\min}$:

$$\omega \le \frac{V}{R_{\min}} \quad . \tag{3}$$

At each time step, the vehicle body covers N nodes of the domain, each of which has a velocity vector of the fluid, e.g. (u_i,v_i) for Point i. The proposed control strategy aims at determining the value of ω aligning the velocity direction of the flow field and the corresponding position on the vehicle body. Equating the velocity ratios, we obtain, for a single point

$$\left(u_i x_i + v_i y_i\right)\omega = v_i V \tag{4}$$

and ω can be calculated directly. However, the vehicle is a rigid body, and the velocity directions are unable to match with the flow field at all points simultaneously. Therefore, the weighted least square method is introduced to optimize ω for best fit. Defining

$$\mathbf{a} = \begin{pmatrix} u_1 x_1 + v_1 y_1 \\ u_2 x_2 + v_2 y_2 \\ \vdots \\ u_n x_n + v_n y_n \end{pmatrix}, \quad \mathbf{b} = \begin{pmatrix} v_1 V \\ v_2 V \\ \vdots \\ v_n V \end{pmatrix}, \quad \mathbf{W} = \begin{pmatrix} w_1 & & & \\ & w_2 & & \\ & & \ddots & \\ & & & w_n \end{pmatrix} \tag{5}$$

the optimal value of ω is calculated through

$$\hat{\omega} = \left(\mathbf{a}^{\mathrm{T}}\mathbf{W}\mathbf{a}\right)^{-1}\mathbf{a}^{\mathrm{T}}\mathbf{W}\mathbf{b} \tag{6}$$

where w_i is the weight of Point i. The use of point weights adds the flexibility to give priority to points near to boundaries, in order to avoid collision. Hence we define

$$w_i = \max\left\{\frac{k}{d_i}, 1\right\} \tag{7}$$

where d_i is the distance from Point i to the nearest wall, and k is a single tunable parameter.

2.4 *Simulation of the vehicle's motion*

With the control method now defined, the vehicle's motion can be simulated, integrating the motion within an inertial coordinate system. Vehicle states are: the global position (X,Y), global yaw angle θ, the velocity of the pivot point relative to the ground V, and the angular speed relative to the ground ω. Since the present study is focusing on the low-speed manoeuvring problem, V can be pre-set as a constant with a sufficiently small value, and ω, which is determined by the steering angle of the steering wheel, can be considered to be directly affected by the input. Therefore the model to simulate the vehicle's motion is

$$\dot{X} = V\cos\theta, \quad \dot{Y} = V\sin\theta, \quad \dot{\theta} = \omega \tag{8}$$

3 SIMULATIONS AND RESULTS

The proposed method is simulated in MATLAB. The parameters used in the vehicle model are based on an MGGS 1.6T experimental vehicle from the Tongji VeCaN lab – see Table 1.

Table 1. Parameter of the vehicle in the simulation

Parameter name	Value	Unit
Length	4.50	m
Width	1.855	m
Front suspension	0.954	m
Rear suspension	0.896	m
R_{min}	4.944	m
δ_{max}	28.18	deg

3.1 *Test cases*

Three cases are considered: (1) Turning left at an intersection; (2) Making a U-turn; (3) Leaving a warehouse from a designated location.

Case 1 is presented in Figure 3(a). The white region represents the road area which is available for the vehicle, and is also the domain for fluid simulation. The vehicle starts heading X+ towards the intersection on its right half of the road. Therefore the inlet boundary of the fluid is located behind the starting point of the vehicle, marked by the red line. The yellow line depicts the outlet boundary of the fluid, which indicates the intended destination of the vehicle. Green arrows throughout the domain stand for the velocity field calculated by the CFD method. By applying the proposed motion control method, the vehicle's path is simulated and plotted as the purple curve. Blue rectangles show the vehicle's postures along the path. It is seen that the vehicle completes its task in a smooth path.

Case 2 considers another common action of the vehicle, making a U-turn. The vehicle starts heading X+ at X=0 on the bottom half of the area, and will make a U-turn to the top half of the area. The inlet boundary and the outlet boundary of the fluid cover the entire width of the available space, implying that the vehicle can start at anywhere on the bottom half, and ending at anywhere on the top half is acceptable. Three simulated paths with different starting positions are plotted in Figure 3 (b). These results also demonstrate that the proposed method can produce smooth paths in such scenario. Furthermore, the flow field needs to be calculated only once, and solutions for different starting points can be obtained from it.

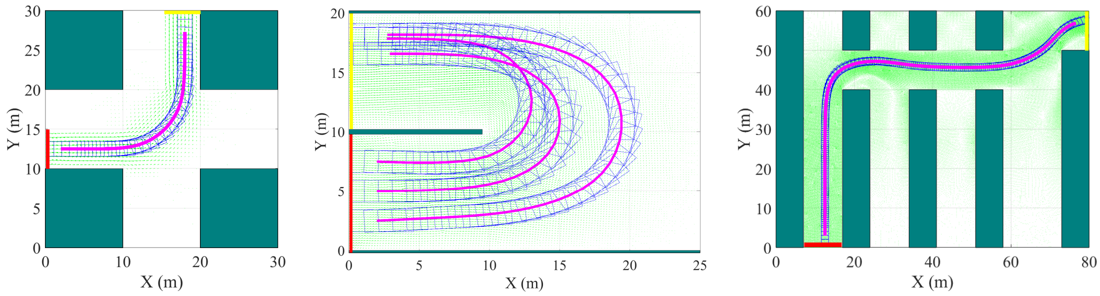

(a) Intersection (b) U-turn (c) Warehouse

Figure 3. Simulated result for the four cases

Case 3 simulates a more complex scenario, where the vehicle is initially parked near the bottom-left corner of the area, and is to leave a warehouse through an exit located near the top-right corner. With mass conservation, the fluid flow nearly stagnates in the areas that do not lead to the exit, while the mainstream automatically finds its way to the destination. Again the vehicle can smoothly reach its destination with the guidance of the flow field.

3.2 *Comparing case with human drivers*

The proposed method is applied to a realistic double-lane-change scenario, and compared with recorded paths produced by real drivers. The experiment was carried out with the experimental unmanned ground vehicle (UGV) of our laboratory (Figure 4 (a)). Sensors installed on the UGV include Light Detection and Ranging (LiDAR), Inertial Measurement Unit (IMU), DGPS (Differential Global Positioning System), and Millimeter-Wave Radar.

This particular test was performed on a straight road as shown in Figure 4 (b). The plan-view is plotted in Figure 5, where three rectangular obstacles enforce the double-lane-change action. The thick pink curve is obtained by the fluid guidance method, while the 8 thin blue curves are experimental results with real human drivers. It can be seen that fluid guidance, while similar to the human drivers, is more symmetrical and more 'careful' to avoid the boundaries.

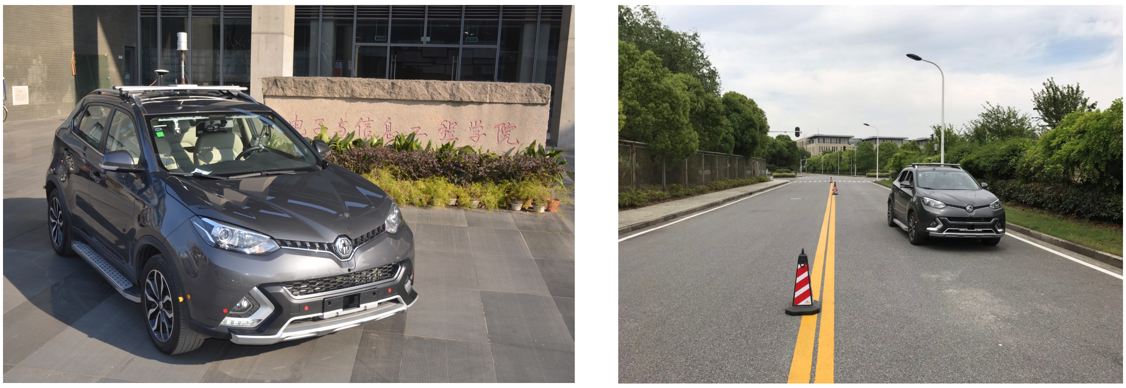
(a) The experimental UGV (b) The testing setup

Figure 4. The experiment setup

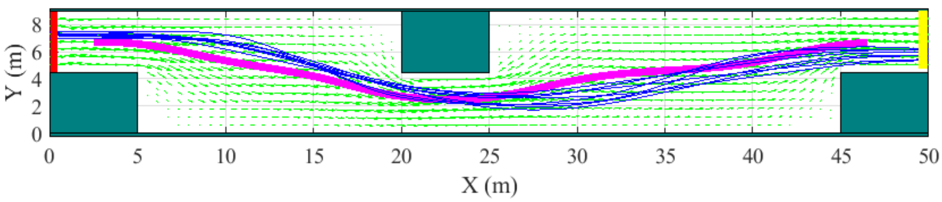

Figure 5. Simulated result for the double-lane-change case

4 CONCLUSIONS

A novel guidance method based on a flow field analogy is proposed for motion control of low-speed manoeuvring of autonomous ground vehicles. The method consists of two layers. On the first layer, the CFD method is introduced to solve a fluid motion problem. The obtained flow field contains velocity vectors all over the domain, providing ubiquitous guidance for the vehicle. Computations in this layer are executed only once for a specific scenario. As a preliminary research in this paper, the control method in the second layer is designed to be as simple as possible as long as it can produce feasible path. This layer uses the discrepancies between the motion of the vehicle body and the motion of the fluid covered by the vehicle body to determine the steering of the vehicle. With the control method and the vehicle model, the path can be generated simultaneously. Simulated results using typical scenarios demonstrate the effectiveness of the proposed method. One particular case, the U-turn, shows that the fluid guidance method can be equally effective for several vehicle starting points, using a single pre-calculated flow field. Future work will evaluate the applicability of the fluid guidance method for dynamic environments (i.e. moving boundaries) and also for multi-vehicle scenarios, where speed control is introduced to avoid vehicle-to-vehicle collisions.

ACKNOWLEDGEMENT

This work was supported by the National Natural Science Foundation of China (NSFC) under Grant No. 61473209.

REFERENCES

Dijkstra, E.W. 1959. A note on two problems in connection with graphs. Numerische Mathematik (1):269–271.

Gordon, T.J., Best, B.C. & Dixon, P.J. 2002. An automated driver based on convergent vector fields. Journal of Automobile Engineering 216(4):329-347.

Gordon, T.J. & Best, M.C. 2006. On the synthesis of driver control inputs for the simulation of handling manoeuvres. International Journal of Vehicle Design 40(1/2/3):52-76.

Hwang, Y.K. & Ahuja, N. 1992. A potential field approach to path planning. IEEE Transactions on Robotics and Automation 8(1):23-32.

Kavraki, L.E. & Svestka, P. 1996. Probabilistic roadmaps for path planning in high-dimensional configuration spaces. IEEE Transactions on Robotics and Automation 12(4):566–580.

LaValle, S.M. & James, J. 2001. Randomized kinodynamic planning. The International Journal of Robotics Research 20(5):378–400.

Likhachev, M. & Ferguson, D.I. 2005. Anytime dynamic A*: An anytime, replanning algorithm. The International Conference on Automated Planning and Scheduling (ICAPS): 262–271.

Phinni, M.J. & Sudheer, A. 2008. Obstacle avoidance of a wheeled mobile robot: A genetic-neurofuzzy approach. IISc Centenary-International Conference on Advances in Mechanical Engineering.

Saffiotti, A. 1997. The uses of fuzzy logic in autonomous robot navigation. Soft Computing 1(4):180–197.

Sedighi, K.H & Ashenayi, K. 2004. Autonomous local path planning for a mobile robot using a genetic algorithm. Evolutionary Computation 2:1338–1345.

Stentz, A. 1994. Optimal and efficient path planning for partially-known environments. IEEE International Conference on Robotics and Automation: 3310–3317.